Two-atom laser

Gordon Yeoman and Georg M. Meyer
Max-Planck-Institut für Quantenoptik, Hans-Kopfermann-Strasse 1, D-85748 Garching, Germany
(Received 2 February 1998)

A theoretical model of a microscopic laser system incorporating two identical atoms coupled to a single resonator mode is investigated in detail. It is established that a dramatic improvement in laser quality results from the addition of a second atom into the cavity. The enhanced laser action, arising from a cavity-induced mutual atomic coherence, is inferred from comprehensive studies of the steady-state and dynamical properties of the cavity output field. Evidence of laser action is also found in the fluorescence field where position-dependent spectral profiles occur. Counterintuitively, we establish that antibunching phenomena in the fluorescence can be enhanced by incoherent pumping. [S1050-2947(98)07709-9]

PACS number(s): 42.50.−p, 32.80.−t, 42.55.−f

I. INTRODUCTION

Recent technical advances in ion traps and laser-cooling schemes coupled with progress in cavity quantum electrodynamics suggest that it may soon be possible to realize microscopic laser systems whose lasing medium consists of only a few atoms. Such a laser system can even involve just a single atom that is cooled to the ground state of its external motion and permanently and strongly coupled to an optical resonator. If the atom is incoherently pumped at a rate that is at least sufficient to compensate for the atomic and cavity losses, it is found that a near-coherent field may accumulate in the resonator via coherent emission into the cavity mode.

A theoretical treatment of the one-atom laser was first performed in Ref. [1]. The practical difficulty of generating an intense laser field with only a single atom as the lasing medium means that the fluctuations in the cavity photon number now play a significant role. As a result, the semiclassical treatment applied to microscopic laser systems is in general no longer valid, thereby requiring the atom-field interaction and the process of cavity loss to be described in a quantum-mechanical manner. By applying the fully quantum model to two-, three-, and four-level atomic systems coupled to a resonator mode, it was shown [1] that a near-coherent field may accumulate in the cavity for particular regimes of pump rate and atom-cavity coupling strength. For such parameters the lasing behavior was inferred from steady-state statistical properties corresponding to a mean cavity photon number greater than unity and a near-Poissonian photon number probability distribution. This was confirmed independently in Ref. [2] by the first calculation of spectral properties of the one-atom two-level laser. A more complete account of the dynamical aspects was later given in Ref. [3]. In addition to laser action, a number of quantum features in the cavity output field such as sub-Poissonian photocounting statistics and intensity squeezing have been predicted. Lasing has also been predicted in the three-level Λ system [4], where good agreement is found between the semiclassical Focker-Planck treatment and the fully quantum description for corresponding effective atom-cavity interaction strengths.

The computational intensity required to investigate one-atom laser systems in the strong-coupling regime suggests that such problems are well-suited to the damping-basis treatment [5] of lossy quantum harmonic oscillators. This approach has been applied to the two-level model of the one-atom laser [2] and found to agree favorably with numerical techniques utilizing the Fock basis. Furthermore, with the help of a pump operator, the damping basis has permitted the study of more realistic multilevel schemes [6]. This effort has resulted in the first proposal for an experimental realization of a one-atom laser in the form of an ion-trap laser [7–9].

The extension of the one-atom laser model to systems incorporating two atoms has been performed in Ref. [10], where three-level atoms with ladder configurations are individually coupled to two resonator modes. The ground-state populations are coherently pumped to the excited state via laser excitation, while the cavity-induced deexcitations between the upper and intermediate states drive the laser mode. Efficient recycling of the atomic populations back to the excited state of the lasing transition is then achieved by interaction with the second cavity mode in the bad-cavity limit followed by a coherent excitation from the lowest atomic state via the applied laser field. The cavity-induced atom-atom correlations lead to a collective atomic behavior similar to that found in free space for small interatomic separation. This leads to a super-radiant behavior that produces an increased photon number occupation of the laser mode at the expense of an increased noise component. A decoupling of the individual atomic recycling processes, achieved by coupling the transition between the intermediate and ground atomic states to different cavity modes, results in a decreased super-radiant effect, yielding a reduced laser intensity but also a less noisy field.

In this paper we shall investigate the simplest model of a two-atom laser [11]; that is, a pair of two-level atoms that are incoherently pumped and coupled to a single lossy resonator mode. We shall compare the two-atom laser with the corresponding one-atom model and establish that the two-atom laser produces light that is closest in character to that of a classical coherent source. In particular, we find that the addition of a second atom into the cavity results in a factor of 4 increase [10] in the maximum allowed mean cavity photon number. Furthermore, a study of the intensity fluctuations reveals that the lasing thresholds are particularly pronounced in the two-atom case and that in the lasing regime the field

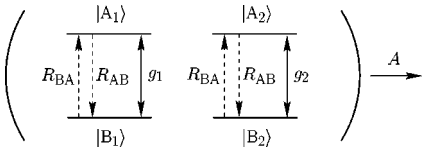

FIG. 1. Schematic representation of the two-atom laser.

statistics most closely resemble a Poisson distribution. The physical origin of these enhancements of the steady-state statistics is explained by introducing an effective gain factor inferred from the atomic population inversion. This theme is continued when we investigate the dynamical properties of the two-atom laser. Lasing action, of course, is not only inferred from steady-state photon number statistics but also from a study of the cavity output spectrum and intensity-intensity correlations [3]. To this end, we calculate and discuss these dynamical quantities. For completeness we also investigate the dynamical behavior of the fluorescence field. Similar to previous studies, the dynamical behaviors of the fluorescence and cavity output fields are found to be qualitatively different. With two-atom systems, however, the feature of position-dependent correlation functions and spectral profiles [12,13] is introduced. This behavior provides a diagnostic of laser action in two-atom systems [11]. Finally, we discuss the surprising result that within the lasing regime, incoherent pumping forms a necessary ingredient to produce antibunching in the fluorescence field. The simple model used to analyze this effect shows that this feature is unique to multiatom systems and arises from atom-atom correlations.

The paper is organized as follows. In Sec. II we establish the two-atom laser model under consideration while in Sec. III we discuss the application of the damping-basis method to two-atom systems and derive the necessary equations of motion. In Sec. IV we investigate the lasing action of our two-atom system by calculation of the field statistics in the steady state. These results are compared with the case of a single atom, and the physical origin of the increased coherent behavior arising in the two-atom model is explained. The dynamical properties of the cavity output and fluorescence fields are investigated in Sec. V. Finally, we conclude the paper with some closing remarks about the experimental realization of microscopic laser systems in the light of recent technical advancements.

II. THE MODEL

In Fig. 1 we establish the system under consideration, namely a pair of two-level atoms that are pumped incoherently with broadband radiation and coherently coupled through their interaction with a single mode of an optical resonator. Within the assumptions that the atoms are sufficiently far apart so that cooperative effects may be ignored and well-localized in space in order to neglect the effect of external motion, the dynamical behavior of the atom-field system is described by the master equation

$$\frac{\partial}{\partial t}\mathrm{P}=\frac{1}{i\hbar}[H,\mathrm{P}]+L_{\mathrm{atom}}\mathrm{P}+L_{\mathrm{field}}\mathrm{P} \tag{1}$$

for the density operator P with the Hamiltonian

$$H=-\hbar g_1(a\sigma_1^\dagger+a^\dagger\sigma_1)-\hbar g_2(a\sigma_2^\dagger+a^\dagger\sigma_2) \tag{2}$$

and the Liouville operators

$$\begin{aligned}L_{\mathrm{atom}}\mathrm{P}=&-\frac{R_{\mathrm{AB}}}{2}(\sigma_1^\dagger\sigma_1\mathrm{P}+\mathrm{P}\sigma_1^\dagger\sigma_1-2\sigma_1\mathrm{P}\sigma_1^\dagger)-\frac{R_{\mathrm{AB}}}{2}(\sigma_2^\dagger\sigma_2\mathrm{P}\\&+\mathrm{P}\sigma_2^\dagger\sigma_2-2\sigma_2\mathrm{P}\sigma_2^\dagger)-\frac{R_{\mathrm{BA}}}{2}(\sigma_1\sigma_1^\dagger\mathrm{P}+\mathrm{P}\sigma_1\sigma_1^\dagger\\&-2\sigma_1^\dagger\mathrm{P}\sigma_1)-\frac{R_{BA}}{2}(\sigma_2\sigma_2^\dagger\mathrm{P}+\mathrm{P}\sigma_2\sigma_2^\dagger-2\sigma_2^\dagger\mathrm{P}\sigma_2),\end{aligned}$$

$$L_{\mathrm{field}}\mathrm{P}=-\frac{A}{2}(a^\dagger a\mathrm{P}+\mathrm{P}a^\dagger a-2a\mathrm{P}a^\dagger), \tag{3}$$

where we have introduced the atomic lowering operators $\sigma_k=|\mathrm{B}_k\rangle\langle\mathrm{A}_k|$ for the kth atom and the field annihilation (creation) operator a $(a^\dagger)$. The interaction strength of each two-level atom with the resonator mode is represented by the vacuum Rabi frequencies g_1 and g_2. Atomic relaxation rates are denoted by the decay rate R_{AB} and the pumping rate R_{BA}, while the photon decay rate is given by A. By allowing the rate of atomic excitation to exceed the rate of decay, our atom-cavity system is extended to the simplest theoretical model of a two-atom laser. Furthermore, our model includes the special case of a one-atom laser [1,2] if we set one of the Rabi frequencies g_1 or g_2 to zero. For the remainder we shall assume for simplicity that $g_1=g_2=g$ unless otherwise stated.

III. TREATMENT OF TWO-ATOM SYSTEMS

A. Damping-basis approach

The state of the atom-field system can be expanded in terms of the bare atomic states and the corresponding conditional field states

$$\mathrm{P}=\sum_{L_1,L_1',L_2,L_2'}\rho_{L_1L_1',L_2L_2'}|L_1,L_2\rangle\langle L_2',L_1'|, \tag{4}$$

where $\rho_{L_1L_1',L_2L_2'}$ describes the state of the field that is associated with the atomic density operator component $|L_1,L_2\rangle\langle L_2',L_1'|$. The conditional field states may be expanded in any convenient basis. In this paper we shall employ the usual Fock basis to investigate the dynamical behavior of our atom-field system. To study the statistical properties in steady state, on the other hand, we shall make use of the recently developed damping basis [5] because the corresponding representation permits the derivation of interesting analytic results. As this latter basis is not as widely known as the Fock basis, we now describe some of its key features.

The damping basis consists of the set of field eigenvectors ρ_λ that fulfill the eigenvalue equation

$$L_{\mathrm{field}}\,\rho_\lambda=\lambda\rho_\lambda\,. \tag{5}$$

In the Fock representation we note that the field damping operator couples only density operator components on the same diagonal; that is, $\langle n|\rho|m\rangle$ is coupled only to $\langle n+1|\rho|m+1\rangle$ and $\langle n-1|\rho|m-1\rangle$. This leads naturally to an ansatz for ρ_λ of the form

$$\rho_\lambda = a^{\dagger(|k|+k)/2} {:} f(a^\dagger a) {:} a^{(|k|-k)/2}, \tag{6}$$

where $:\cdots:$ denotes normal ordering. This ansatz, together with the condition that the expectation value of any observable be finite, results in the eigenvalues

$$\lambda_n^{(k)} = -A(n+|k|/2) \tag{7}$$

and corresponding eigenvectors

$$\rho_n^{(k)} = a^{\dagger(|k|+k)/2}(-1)^{a^\dagger a+n}\begin{pmatrix} n+|k| \\ a^\dagger a+|k| \end{pmatrix} a^{(|k|-k)/2}, \tag{8}$$

where $n=0,1,2,\ldots$ and $k=0,\pm1,\pm2,\ldots$ [5]. A similar procedure may also be followed to find the dual eigenvectors satisfying $\check{\rho}_n^{(k)} L_{\text{field}} = \lambda_n^{(k)} \check{\rho}_n^{(k)}$.

For the two-atom case considered in this paper we now make the following expansions in the damping basis:

$$\rho_{L_1L_1',L_2L_2'} = \sum_{n,k} \alpha_{nk}^{L_1L_1',L_2L_2'} \rho_n^{(k)} \tag{9}$$

for all L_1L_1', L_2L_2' that describe two populations, and

$$\rho_{L_1L_1',L_2L_2'} = \sum_{n,k} \alpha_{nk}^{L_1L_1',L_2L_2'} \rho_n^{(k-1)},$$

$$\rho_{L_1L_1',L_2L_2'} = \sum_{n,k} \alpha_{nk}^{L_1L_1',L_2L_2'} \rho_n^{(k+1)} \tag{10}$$

for all L_1L_1', L_2L_2' that describe one population (AA or BB) and one polarization (AB or BA). When the labels describe two atomic polarizations of the same orientation we choose

$$\rho_{\text{AB,AB}} = \sum_{n,k} \alpha_{nk}^{\text{AB,AB}} \rho_n^{(k-2)}, \tag{11}$$

$$\rho_{\text{BA,BA}} = \sum_{n,k} \alpha_{nk}^{\text{BA,BA}} \rho_n^{(k+2)},$$

while for two polarizations of opposite orientations we employ the expansions

$$\rho_{\text{AB,BA}} = \sum_{n,k} \alpha_{nk}^{\text{AB,BA}} \rho_n^{(k)},$$

$$\rho_{\text{BA,AB}} = \sum_{n,k} \alpha_{nk}^{\text{BA,AB}} \rho_n^{(k)}. \tag{12}$$

By substituting the expansions (9)–(12) into Eq. (1), equations of motion for the coefficients $\alpha_{nk}^{L_1L_1',L_2L_2'}$ may be derived by tracing over the dual vector

$$\alpha_{nk}^{L_1L_1',L_2L_2'} = \text{Tr}[\check{\rho}_n^k \rho_{L_1L_1',L_2L_2'}]. \tag{13}$$

These specific substitutions are made so that the equations of motion for the expansion coefficients couple only to terms with the same k. It is particularly important to achieve coupled equations of this form because in the stationary state the only nonvanishing contributions arise from the $k=0$ subset. This is a direct result of the fact that field damping will destroy phase-sensitive expectation values such as $\langle a\rangle$, $\langle a^2\rangle$, etc.

Solution of the $k=0$ subset in the steady state yields the field moments of our laser system. For example, it has been shown [5] that the first and second field moments are given by

$$\langle a^\dagger a\rangle = \alpha_{10},$$

$$\langle (a^\dagger a - \langle a^\dagger a\rangle)^2\rangle = 2\alpha_{20} - \alpha_{10}^2 + \alpha_{10}, \tag{14}$$

where, for our two-atom system, α_{n0} is found by a simple trace operation with the result

$$\alpha_{n0} = \alpha_{n0}^{\text{AA,AA}} + \alpha_{n0}^{\text{BB,BB}} + \alpha_{n0}^{\text{AA,BB}} + \alpha_{n0}^{\text{BB,AA}}. \tag{15}$$

B. Equations of motion

The equations of motion for the $k=0$ subset in the damping basis have the form

$$\frac{\partial}{\partial t} X_n = M_n X_n + F_n X_{n-1} + G_n X_{n+1}, \tag{16}$$

where

$$X_n = \begin{pmatrix} \alpha_{n0}^{\text{AA,AA}} \\ \alpha_{n0}^{\text{BA,AA}} - \alpha_{n0}^{\text{AB,AA}} + \alpha_{n0}^{\text{AA,BA}} - \alpha_{n0}^{\text{AA,AB}} \\ \alpha_{n0}^{\text{AB,AB}} + \alpha_{n0}^{\text{BA,BA}} \\ \alpha_{n0}^{\text{AA,BB}} + \alpha_{n0}^{\text{BB,AA}} \\ \alpha_{n0}^{\text{AB,BA}} + \alpha_{n0}^{\text{BA,AB}} \\ \alpha_{n0}^{\text{BB,BA}} - \alpha_{n0}^{\text{BB,AB}} + \alpha_{n0}^{\text{BA,BB}} - \alpha_{n0}^{\text{AB,BB}} \\ \alpha_{n0}^{\text{BB,BB}} \end{pmatrix} \tag{17}$$

and

$$M_n=\begin{pmatrix} -\gamma_1 & ig(n+1) & 0 & R_{\rm BA} & 0 & 0 & 0 \\ 4ig & -\gamma_2 & 2ig(n+2) & 0 & 0 & R_{BA} & 0 \\ 0 & ig & -\gamma_3 & 0 & 0 & 0 & 0 \\ 2R_{AB} & -ig(n+1) & 0 & -\gamma_4 & 0 & ig(n+1) & 2R_{\rm BA} \\ 0 & -ig(n+1) & 0 & 0 & -\gamma_5 & ig(n+1) & 0 \\ 0 & R_{\rm AB} & -2ig(n+2) & 2ig & 2ig & -\gamma_6 & 0 \\ 0 & 0 & 0 & R_{\rm AB} & 0 & -ig(n+1) & -\gamma_7 \end{pmatrix}, \tag{18}$$

$$F_n=ign\begin{pmatrix} 0 & 0 & 0 & 0 & 0 & 0 & 0 \\ 0 & 0 & 0 & 0 & 0 & 0 & 0 \\ 0 & 0 & 0 & 0 & 0 & 0 & 0 \\ 0 & -1 & 0 & 0 & 0 & 0 & 0 \\ 0 & -1 & 0 & 0 & 0 & 0 & 0 \\ 0 & 0 & -2 & 0 & 0 & 0 & 0 \\ 0 & 0 & 0 & 0 & 0 & -1 & 0 \end{pmatrix}, \tag{19}$$

$$G_n=ig\begin{pmatrix} 0 & 0 & 0 & 0 & 0 & 0 & 0 \\ 4 & 0 & 0 & -2 & -2 & 0 & 0 \\ 0 & 1 & 0 & 0 & 0 & -1 & 0 \\ 0 & 0 & 0 & 0 & 0 & 0 & 0 \\ 0 & 0 & 0 & 0 & 0 & 0 & 0 \\ 0 & 0 & 0 & 2 & 2 & 0 & -4 \\ 0 & 0 & 0 & 0 & 0 & 0 & 0 \end{pmatrix},$$

with the relaxation rates

$$\gamma_1=An+2R_{\rm AB},$$

$$\gamma_2=A(n+1/2)+R_{\rm AB}+\gamma_{\rm AB},$$

$$\gamma_3=A(n+1)+2\gamma_{\rm AB},$$

$$\gamma_4=An+R_{\rm AB}+R_{\rm BA},$$

$$\gamma_5=An+2\gamma_{\rm AB},$$

$$\gamma_6=A(n+1/2)+R_{\rm BA}+\gamma_{\rm AB},$$

$$\gamma_7=An+2R_{\rm BA}. \tag{20}$$

Here $\gamma_{\rm AB}$ is the transverse relaxation rate of the two-level atoms. In the absence of additional (e.g., collisional) phase decay, the relation $\gamma_{\rm AB}=(R_{\rm AB}+R_{\rm BA})/2$ holds.

We note that by employing a particular basis for the calculation, we are able to reduce the expected 16×16 matrices for pairs of two-level atomic systems to the 7×7 forms shown in Eqs. (18) and (19). This reduction in the damping-basis treatment has a particular significance as it permits the derivation of analytical results in particular parameter regimes. For example, for a small pump rate $R_{BA}\ll R_{AB}$ the steady-state problem can be simplified to equations involving only the vectors X_0 and X_1. By solving this reduced set of equations, quantities such as the fringe visibility of the fluorescence field [11] and cavity-induced atomic decay rates [12] may be derived analytically. Details of these calculations are provided in the Appendix. We finally note that the reduction to 7×7 matrices is possible only for the case $g_1=g_2=g$. For $g_1\neq g_2$ an appropriate choice of the basis is found to result in 10×10 matrices.

C. Matrix-continued fractions

We now outline the technique of matrix-continued fractions used to calculate numerically the expansion coefficients in the stationary state. This is achieved by setting the left-hand side of Eq. (16) to zero and assuming a solution of the form

$$X_{n+1}=R_nX_n. \tag{21}$$

Substitution of Eq. (21) into Eq. (16) provides a recursive relationship

$$R_{n-1}=-(M_n+G_nR_n)^{-1}F_n. \tag{22}$$

It is then possible to iterate backwards and calculate all the matrices R_n provided that we truncate the solution at some suitably large value $n=n_{\rm max}$ by imposing the condition

$$X_{n_{\rm max}}=R_{n_{\rm max}-1}=0. \tag{23}$$

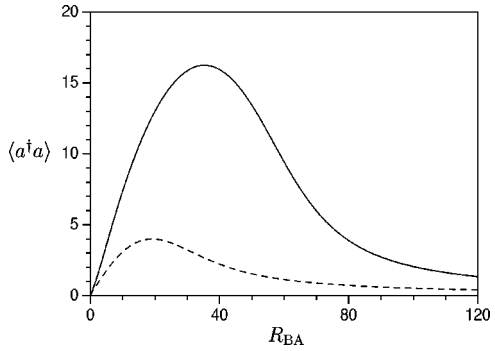

FIG. 2. Mean photon number $\langle a^\dagger a \rangle$ for $R_{AB}=1$ and $g=3$. The two-atom laser with $g_1=g_2=g$ (solid) is compared to the one-atom laser with $g_1=g$ and $g_2=0$ (dashed). All rates are in units of A.

After we have iterated backwards from $n=n_{\max}$ to $n=0$, we calculate the vector X_0 by imposing the normalization condition $\alpha_{00}=1$ onto the degenerate set of equations

$$(M_0+G_0R_0)X_0=0. \tag{24}$$

It is now a simple task to calculate all the remaining solutions X_n by forward iteration with the aid of Eq. (21).

IV. TWO-ATOM LASING

To investigate the field properties of our laser system in the steady state we consider the mean cavity photon number $\langle a^\dagger a \rangle$, and the intensity fluctuations described by the Fano factor

$$F=\frac{\langle (a^\dagger a-\langle a^\dagger a\rangle)^2\rangle}{\langle a^\dagger a\rangle}. \tag{25}$$

Taken together, these quantities provide a broad account of the quality of a laser field by describing not only the field intensity but also its coherent character, which is reflected in the photon number probability distribution. The numerical calculations of these observables are performed in the damping basis using the matrix-continued fraction technique outlined in the preceding section.

To begin our discussion of the steady-state field properties, we focus on the mean cavity photon number. In Fig. 2 we plot this quantity as a function of the pumping rate R_{BA} for the atom-cavity parameters $R_{AB}=1$ and $g_1=g_2=g=3$ with all rates in units of A. As a reference, we also show the field statistics for the one-atom case with identical atomic and cavity characteristics.

Inspection of Fig. 2 reveals that the field intensity of the two-atom laser system is qualitatively similar to that found for one atom. In both cases the mean photon number rises approximately linearly with increasing pumping rate until some critical value of R_{BA} is reached. For pump rates above this critical value, the photon numbers decrease and approach zero. Quantitatively, however, the behavior of the two-atom system is markedly different from the one-atom case. In particular, we observe that the maximum cavity photon number in the two-atom laser is approximately four times that found in the one-atom case. Further numerical studies show that this factor remains approximately constant in the region $g>R_{AB},A$. To explain this result we must first consider the physical mechanisms that lead to the production of cavity laser fields.

For the case of a single atom, the atom-cavity system acts as a lasing medium only when the pump is sufficiently strong to induce a population inversion, but not so strong that it destroys the coherence between the atom and the cavity mode. For these intermediate pump strengths, the coherent atom-cavity coupling can precipitate a single stimulated emission per atomic excitation. Provided that a population inversion can be regenerated by continuous pumping, a coherent field builds up in the cavity via a sequence of such stimulated emissions. This model may be extended to two atoms except that in this case the atom-cavity coupling now precipitates *two* stimulated emissions into the cavity if both atoms are initially excited. From this simple heuristic analysis we deduce that in the lasing regime, where strong atomic inversions and atom-cavity couplings coexist, the two-atom laser may be assigned an effective gain factor $2G$, where G is the gain of the one-atom system. Thus, for a given pump rate Γ, the number of cavity photons will be proportional to $2G\Gamma$ for the two-atom case and $G\Gamma$ for a single atom.

The maximum number of photons allowed in the cavity finally depends on the largest value of R_{BA} at which significant atom-cavity coupling and the attendant linear gain persist. The coupling strength is described by the cooperativity parameter defined as $\Sigma_k g_k^2/A(R_{AB}+R_{BA})$, where g_k is the vacuum Rabi frequency of the kth atom. By assuming that there is a minimum value of the cooperativity parameter below which lasing action ceases, it is trivial to show that for two atoms this occurs at approximately $2P$ if P denotes the pump strength at which one-atom lasing terminates. This prediction is confirmed by inspection of Fig. 2. Consequently, a factor of roughly four $[=(2G)(2P)/(GP)]$ more photons may be produced in the two-atom laser than in the one-atom laser for identical atomic and cavity characteristics.

Having discussed the field intensity of the two-atom laser, it is important to consider the intensity fluctuations by calculating the Fano factor. The Fano factor F is simply the ratio of the photon number variance and mean as shown in Eq. (25). Thus, a Fano factor of greater than unity indicates a super-Poissonian photon number distribution while a value less than unity indicates a sub-Poissonian distribution. Coherent fields, on the other hand, are characterized by having a Poissonian photon number probability distribution and a Fano factor equal to unity.

In Fig. 3 we plot the Fano factor F for the one- and two-atom lasers as functions of the pump strength R_{BA} for the parameters employed in Fig. 2. We first identify the lasing regime in both cases as the pump region in-between the two lasing thresholds, represented by the first and second maxima. Within the lasing regime the cavity fields have mean photon numbers much greater than unity and photon number distributions that are approximately Poissonian, indicating that a near-coherent field is present.

For the two-atom case we observe that the first threshold for lasing is much more pronounced compared with the situation where only one atom couples to the cavity mode. The reason for this pronounced behavior is explained by first understanding the source of incoherence in lasers operating below threshold. Below threshold the rate of excitation is small

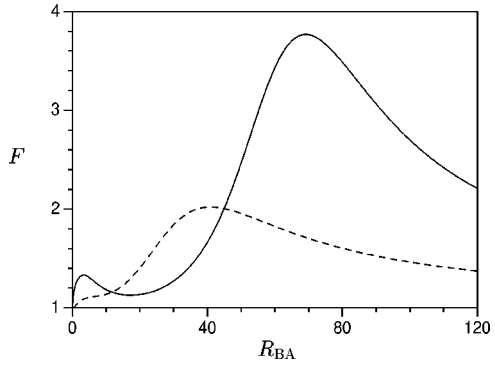

FIG. 3. Fano factor F for $R_{AB}=1$ and $g=3$. The two-atom laser with $g_1=g_2=g$ (solid) is compared to the one-atom laser with $g_1=g$ and $g_2=0$ (dashed). All rates are in units of A.

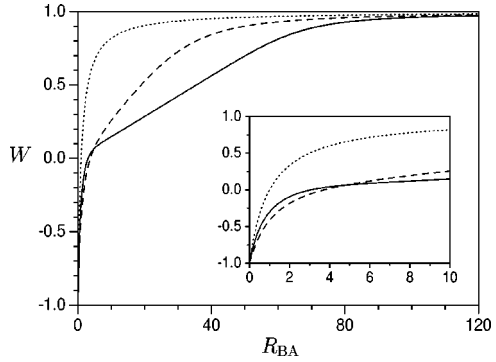

FIG. 4. Atomic inversion W versus the pump rate R_{BA} for $R_{\mathrm{AB}}=1$ and $g=3$. The inversion of each individual atom of the two-atom laser with $g_1=g_2=g$ (solid) is compared to the inversion for the one-atom laser (dashed) and to a single atom not coupled to a cavity (dotted). All rates are in units of *A*.

with respect to the photon decay rate so that the resonator mode is unable to store photons in-between successive atomic pump processes. Successive stimulated emissions into the cavity mode are therefore uncorrelated, leading to the buildup of noise in the resonator. A two-atom laser model thus produces a more incoherent field below threshold as it contains double the number of noise sources compared to the case of one atom in an identical cavity, even when the vacuum Rabi frequency of the single-atom laser is rescaled to $\sqrt{2}g$. This naturally results in a cavity field that is more *incoherent*. Above threshold, we find that our two-atom model generates a field that is more *coherent* in character. The reason for this is simply that two atoms produce a larger atom-cavity coupling strength. This is reflected in the eigenvalues $\pm\sqrt{2}g$ of the two-atom Tavis-Cummings Hamiltonian compared to $\pm g$ arising from the Jaynes-Cummings Hamiltonian for a single atom. As a result, a longer sequence of stimulated emissions may occur before noise attributed to the photon decay rate is allowed to accumulate. Two atoms will thus lead to a field that is more coherent in character, thereby producing a Fano factor closer to unity. It is the combination of these two effects of increased incoherent emissions into the cavity below threshold and a stronger effective Rabi frequency above that lead to a more pronounced lasing threshold for the two-atom case.

For pump strengths beyond the individual Fano minima we find that both curves of Fig. 3 rise rapidly until they reach their respective maxima. The reason for the increase is simply that although the increased pump produces a rise in the atomic inversion, its effect is overwhelmed by the destruction of the atom-cavity coherence. The increased pump rates permitted by the two-atom system before the coherence is completely diminished naturally produce a maximum in the Fano factor at higher values of R_{BA}. The maximum value of the Fano factor for large R_{BA} is found to be greater for 2 atoms because we now have twice the number of incoherent sources emitting into the resonator mode, similar to the behavior found below the first lasing threshold. Beyond the second maxima, the Fano factors decrease in step with the reduction in cavity photon number, leading the cavity field to the vacuum state with Fano factor equal to unity.

Many of the features of the mean cavity photon number and Fano factor are manifest in the atomic inversion for the kth atom $W_k=\langle[\sigma_k^{\dagger},\sigma_k]\rangle$. For symmetric pumping and atom-cavity coupling we find that $W_1=W_2=W$, the quantity shown in Fig. 4. We first observe that the region between the lasing thresholds of Fig. 3 coincide with a linear region of atomic inversion for both the one- and two-atom cases. This, of course, provides a confirmation of the linear response of the lasing medium invoked to explain the increased cavity photon number in our two-atom system. The relative gain factors of the two models may also be ascertained from the atomic inversion. In the linear region we find that the gradient of the inversion for two atoms is roughly half that for one atom, indicating that the atomic excitation is twice as efficiently depleted through stimulated emission into the resonator. The gain factor is thus a factor of two higher in the two-atom case compared with the one-atom laser. Finally, we note that the region in which the atomic inversion increases linearly with pumping rate is twice as long for the two-atom case as for one atom. This coincides with the higher pump rates permitted by two atoms before the atom-cavity coherence is destroyed.

The steady-state properties presented here suggest that the two-atom model has characteristics that are more laserlike than the one-atom case. For example, the gain in the lasing region is closer to a linear response for two atoms than in the presence of only one. Furthermore, a field with a distribution closer to Poissonian and with greater intensity results. The field generated by the two-atom laser is thus closer in its behavior to that of a classical coherent field. This theme continues in the dynamical properties of the one- and two-atom laser systems.

V. DYNAMICAL PROPERTIES

In this section we shall discuss the dynamical properties of the two-atom lasing system under consideration. In particular, we shall focus on the spectral profiles and intensity correlations of the fluorescence and cavity output fields. Throughout, we shall concentrate on the above-threshold parameter regimes, which give rise to a cavity laser field. The dynamical behavior below the laser threshold has previously been studied in detail in Ref. [12].

A. Spectrum

The atom-cavity system under consideration gives rise to two distinct and measurable spectra arising separately from

atomic and cavity relaxation. In the far field and in the steady state, the fluorescence spectrum, $S_\sigma(\omega)$, and the cavity output spectrum, $S_a(\omega)$, arising from these two processes have the definitions

$$S_\sigma(\omega)=\int_0^\infty d\tau\cos[(\omega-\omega_0)\tau]g_\sigma(\tau),$$
$$S_a(\omega)=\int_0^\infty d\tau\cos[(\omega-\omega_0)\tau]g_a(\tau), \tag{26}$$

where

$$g_\sigma(\tau)=\sum_{k=1}^{2}\sum_{l=1}^{2}\langle\sigma_k^\dagger(\tau)\sigma_l(0)\rangle_{\rm ss}\exp[i\varphi(k-l)],$$
$$g_a(\tau)=\langle a^\dagger(\tau)a(0)\rangle_{\rm ss}. \tag{27}$$

The parameter φ is a phase describing the position of the detector with respect to the line center and is given by $\varphi=\omega_0 x/c$, where x denotes the displacement of the detector from the symmetry plane perpendicular to the line connecting the two atoms. The quantities ω_0 and c are constants representing the atomic transition frequency and the speed of light in vacuum, respectively. Thus, $\varphi=0$ corresponds to a position at which the optical path length from each atom is identical. On the other hand, positions where the optical path lengths differ by half of a cavity wavelength are represented by $\varphi=\pi$.

In Fig. 5 we show the fluorescence spectra that occur at positions $\varphi=0$ and $\varphi=\pi$ for the parameters $R_{\rm AB}=A=1$, $g=10$, and $R_{\rm BA}=20$. For these parameters it may be shown that a near-coherent field accumulates in the cavity, similar to the behavior found in Figs. 2–4. Consequently, we may effectively replace the atom-cavity system of Fig. 1 with the semiclassical system of two atoms coherently driven by strong fields of the same phase and incoherently pumped with broadband radiation of random phase. It is well established that a single atom that is coherently driven by a strong field radiates a fluorescence spectrum composed of an elastically scattered δ-function peak along with a three-peaked structure, known as the Mollow triplet [14], arising from inelastic scattering processes. The addition of an incoherent pump to this simple system serves only to broaden the three near-Lorentzian Mollow peaks. For the case of two atoms we expect a similar behavior with the exception that the scattered coherent light forms the basis of a Young-type interference experiment [15–17].

At the line center ($\varphi=0$) the coherent components of the scattered light will experience constructive interference while at $\varphi=\pi$ canceling through destructive interference will occur. The inelastically scattered light does not experience position-dependent constructive or destructive quantum interference due to the random phase of this emitted radiation. Thus, the detection of the identical triplet profiles inelastically scattered by each atom is independent of position. The spectral profile measured at the line center will then consist of three broadened near-Lorentzian peaks together with an approximate δ-function component centered on the natural atomic frequency. The width of the peaks of the Mollow triplet will be of the order of $R_{\rm BA}$ for pump rates much

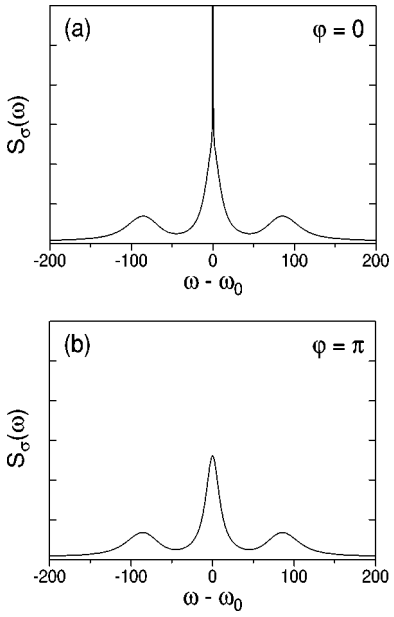

FIG. 5. Fluorescence spectra for a two-atom laser at positions (a) $\varphi=0$ and (b) $\varphi=\pi$ for $R_{\rm AB}=1$, $g=10$, and $R_{\rm BA}=20$ with all parameters in units of A.

greater than the natural atomic linewidth. This behavior is shown in Fig. 5(a). As we move away from the line center the inelastically scattered component of the fluorescent spectrum will remain unchanged while the height of the elastic peak will diminish through increasing destructive interference. Eventually, at $\varphi=\pi$, total cancelation of the coherently scattered light occurs and the remaining spectrum is simply the broadened Mollow triplet. This case is depicted in Fig. 5(b).

The laser output spectrum has a behavior that is quite different from the fluorescence spectrum. As might be expected, the build-up of a near-coherent field in the cavity is accompanied by an intensity spectrum that closely resembles a δ-like Lorentzian. This behavior occurs for both one- and two-atom laser systems, although with different widths occurring for different parameters. Of more interest is a comparison of the spectral widths from the two different atom-cavity systems. With this in mind we plot in Fig. 6 the full

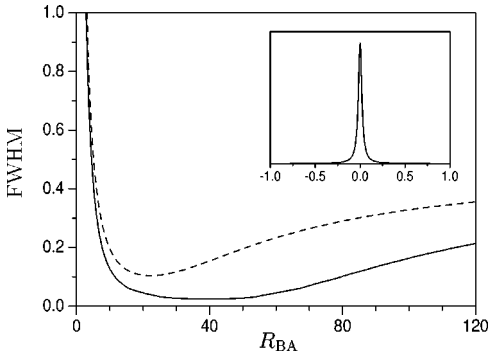

FIG. 6. Full width at half maximum (FWHM) as a function of $R_{\rm BA}$ for the two-atom laser (solid) and the one-atom laser (dashed) for $R_{\rm AB}=1$ and $g=3$. The inset shows the cavity output spectrum $S_a(\omega)$ for the two-atom laser with $R_{\rm BA}=40$. All parameters are in units of A.

width at half maximum of the single-peaked output laser spectrum as a function of the pump rate for equivalent one- and two-atom laser models. Here, of course, we consider only the pumping regime beyond the first lasing threshold where a single peak occurs. So that we may compare the plot with the steady-state results of the preceding section, we employ the same atom-cavity parameters as in Figs. 2 and 3.

By comparison of Fig. 6 with Fig. 3, we observe that the pump rates that minimize the spectral widths also coincide with Fano factor minima for both one- and two-atom systems. This, of course, is to be expected as coherence is characterized not only by the photon number distribution being Poissonian but also by a well-defined phase and therefore a narrow spectral width. Second, we note that the two-atom laser model gives rise to narrower laser peaks than the one-atom laser when the same atom-cavity parameters are employed. Closer inspection shows that the narrowest peak permitted in the two-atom laser model is approximately one-quarter of that found with one atom. This provides further confirmation of the $\langle a^{\dagger}a\rangle^{-1}$ dependence of the laser linewidth [9] in microscopic lasers. In addition, this finding reinforces our theme of improved laser equality with multiatom systems.

B. Intensity-intensity correlations

Similar to the spectral profiles, the intensity-intensity correlations of the two-atom laser may be separately measured in the fluorescence and cavity output fields. These statistical measures are described by the normalized second-order correlation function for the fluorescence field, $g_{\sigma}^{(2)}(\tau)$, and for the laser output, $g_{a}^{(2)}(\tau)$, defined as

$$g_{\sigma}^{(2)}(\tau)=\frac{G_{\sigma}^{(2)}(\tau)}{[g_{\sigma}(0)]^2},$$

$$g_{a}^{(2)}(\tau)=\frac{G_{a}^{(2)}(\tau)}{[g_{a}(0)]^2}, \tag{28}$$

where

$$G_{\sigma}^{(2)}(\tau)=\sum_{k,l,m,n=1}^{2}\langle\sigma_k^{\dagger}(0)\sigma_l^{\dagger}(\tau)\sigma_m(\tau)\sigma_n(0)\rangle_{\rm ss}\times\exp[i\varphi(k+l-m-n)],$$

$$G_{a}^{(2)}(\tau)=\langle a^{\dagger}(0)a^{\dagger}(\tau)a(\tau)a(0)\rangle_{\rm ss}. \tag{29}$$

In Fig. 7 we plot the normalized second-order correlation function of the fluorescence field for the parameters $R_{\rm AB}=A=1$, $g=3$, $R_{\rm BA}=20$ at positions corresponding to $\varphi=0$ and π. Similar to the spectral profiles of the fluorescence field, we find that the intensity-intensity correlations are strongly dependent on position. In particular, we observe that for short delay times the fluorescence field displays antibunched statistics at the line center while bunching is found at $\varphi=\pi$. This behavior is found to persist for parameters that allow a near-coherent field to accumulate in the cavity. Consequently, this effect may be explained by invoking the semiclassical picture of two atoms that are simultaneously coherently and incoherently pumped, as previously discussed in connection with the fluorescence spectrum.

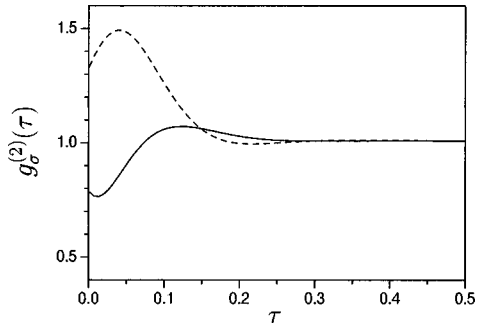

FIG. 7. Second-order correlation function of the fluorescence field from a two-atom laser at $\varphi=0$ (solid) and $\varphi=\pi$ (dashed) for $R_{\rm AB}=1$, $g=3$, and $R_{\rm BA}=20$ with all parameters in units of A.

When a single atom is strongly driven with coherent light and damped by spontaneous emission into the vacuum, the steady-state population is distributed approximately equally between the ground and excited state. Extending this behavior to two atoms gives rise to equal populations of each of the Dicke states $|{\rm B}_1,{\rm B}_2\rangle$, $|{\rm A}_1,{\rm A}_2\rangle$, and $|\pm\rangle=(|{\rm A}_1,{\rm B}_2\rangle \pm|{\rm B}_1,{\rm A}_2\rangle)/\sqrt{2}$. The addition of a strong incoherent pump has the effect of depleting the population that accumulates in the antisymmetric state by excitation to the doubly excited state $|{\rm A}_1,{\rm A}_2\rangle$. The population of the symmetric states $|{\rm B}_1,{\rm B}_2\rangle$ and $|+\rangle$ are also depleted by the action of the incoherent pump. In contrast to the antisymmetric state, however, these states are at least partially repopulated by the coherent coupling, induced by the near-coherent cavity field, which exists between the three symmetric states. Consequently, an asymmetry in the populations of the singly excited Dicke states occurs in the lasing regime. This has a profound effect on the intensity-intensity correlations. For example, the relatively low occupation of the antisymmetric state means that a photodetection event at $\varphi=\pi$ is more likely to correspond to the decay process $|{\rm A}_1,{\rm A}_2\rangle\rightarrow|-\rangle$ than $|-\rangle\rightarrow|{\rm B}_1,{\rm B}_2\rangle$ (in the case $R_{\rm BA}=0$ these events will, of course, be equally probable). The remaining atomic excitation means that there is a strong possibility of immediately registering a subsequent detection event at the same position, thereby producing bunched photocounting statistics. The field statistics at $\varphi=0$, on the other hand, display antibunched characteristics. The increased population of $|+\rangle$ relative to its antisymmetric counterpart means that there is now a stronger probability of an initial photocount projecting the two-atom system onto the ground state $|{\rm B}_1,{\rm B}_2\rangle$. Thus, there is an increased probability that no subsequent photocount can be recorded. This behavior leads to antibunched statistics characterized by $g^2(0)<1$. Similar to single-atom resonance fluorescence [18], inspection of Fig. 7 reveals that the second-order correlation function is modulated at the Rabi frequency and decays at the rate of incoherent excitation. From our argument, we conclude that the antibunching behavior at $\varphi=0$ will become less pronounced as R_{BA} decreases as the population of the $|\pm\rangle$ states will become more equal. Therefore, we see that incoherent excitation is a necessary ingredient for the detection of antibunched statistics in the regime of strong coherent driving.

To complete our discussion of the intensity-intensity cor-

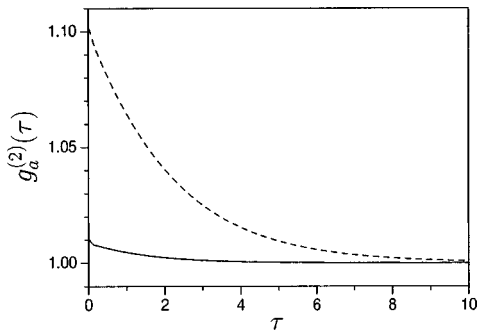

FIG. 8. Second-order correlation function of the cavity output field from the two-atom laser (solid) and the one-atom laser (dashed) for $R_{AB}=1$, $g=3$, and $R_{BA}=20$ with all parameters in units of A.

relations of the two-atom laser, we now consider the statistics of the cavity output field. In Fig. 8 we plot $g_a^{(2)}(\tau)$ for the outputs of both one- and two-atom systems for the parameters corresponding to Fig. 7. We note here that the two-atom and one-atom lasers display second-order correlation functions similar to that characteristic of coherent light as their values are close to unity. Furthermore, in keeping with the previously noted behavior, we find that for identical parameters the two-atom laser exhibits behavior that most closely resembles that of classical coherent light.

VI. CONCLUSIONS

It has recently been demonstrated that pairs of ions may be trapped, cooled, and stored with a level of stability sufficient to perform a Young-type interference experiment [15] where two-level atomic systems replace the slits of Young's original experiment. Indeed, in tests of cooperative phenomena [19] it has been shown in practice that atom pairs may be stored with interatomic separations of the order of an optical wavelength. To date, a number of practical and ingenious schemes such as quantum logic devices [20] and improved frequency standards [21] have been proposed that exploit the unique environment presented by trapped and cooled ions. As sources of localized multiatom systems become more readily available, questions relating to their behavior and other possible applications become pertinent. For instance, an experiment to determine which-way information by employing two atoms has been suggested in Ref. [22].

In this paper we have extended the theory of the one-atom laser to incorporate a second identical atom. The theory of the one-atom laser has reached a stage of development where realizable experimental schemes have been proposed that utilize multilevel but single-atom systems with an array of pumps and coherences. However, the central difficulty in the realization of microscopic laser systems remains rooted in the strength of the atom-cavity coherence that is required to produce lasing action. With the advancements in trapping technology in mind, it seems sensible to attempt to increase this interaction strength via the atom-atom correlations that occur when two atoms are coupled to the same resonator mode. We have shown, in agreement with Ref. [10], where the lasing transition was coherently pumped, that the simple addition of a second atom leads to a factor of 4 increase in the allowed mean cavity photon number. This increase is found to coincide with a significantly more pronounced coherent behavior reflected in the laser linewidth and the photon number probability distribution. All of this suggests that new generations of linear ion traps, able to store a large number of ions at a potential minimum, may provide the key to the development of microscopic sources of laser light.

ACKNOWLEDGMENT

G.Y. acknowledges financial support by the European TMR Network under Grant No. ERB-FMRX-CT96-0087.

APPENDIX A: ANALYTICAL RESULTS

Here we outline the method used to derive the analytical results of Ref. [11]. In Ref. [11] it was established that for weak incoherent pump rates, that is, below the laser threshold, the fluorescence field displays an intensity minimum at the line center, characterized by the quantity

$$C=\frac{\langle\sigma_1^\dagger\sigma_2+\sigma_2^\dagger\sigma_1\rangle_{ss}}{\langle\sigma_1^\dagger\sigma_1+\sigma_2^\dagger\sigma_2\rangle_{ss}} \tag{A1}$$

having negative values. Furthermore, for particularly weak pumps $R_{BA}\ll R_{AB},g$ the fringe contrast factor C has an exact analytical solution. This result is derived by solving the matrix equation (16) and then applying the limit $R_{BA}\to 0$. The key to this derivation is that the probability of the atom-cavity system having two or more excitation quanta is negligible for particularly weak pumps. Therefore, we need only solve for the vectors X_0 and X_1 as the components of all the remaining vectors will have values that rapidly tend towards zero in the limit under consideration.

In the steady state, the remaining set of linear equations may be expressed in the following form:

$$\Lambda Y=0, \tag{A2}$$

where

$$\Lambda=\left(\begin{array}{c|c} M_0 & G_0 \\ -- & -- \\ F_1 & M_1 \end{array}\right) \tag{A3}$$

and

$$Y=\left(\begin{array}{c} Y_1 \\ Y_2 \\ \vdots \\ Y_{14} \end{array}\right)=\left(\begin{array}{c} X_0 \\ -- \\ X_1 \end{array}\right). \tag{A4}$$

Before solving this 14×14 problem, we note that there exists a degeneracy in the equations involving M_0 and G_0. To obtain a unique solution, we simply remove one of the degenerate equations and substitute the normalization condition

$$\alpha_{00}^{AA,AA}+\alpha_{00}^{BB,BB}+\alpha_{00}^{BB,AA}+\alpha_{00}^{AA,BB}=1 \tag{A5}$$

in its place. By using standard techniques of linear algebra,

the components of the vector Y may now be found as functions of the system parameters g, A, R_{AB}, and R_{BA}. These solutions, of course, are only valid for $R_{BA} \ll R_{AB}, g$. We now generate the final exact solution for the fringe contrast factor in the limit of weak incoherent pumping by applying the limit $R_{BA} \to 0$ to C,

$$\lim_{R_{BA}\to 0} C = \lim_{R_{BA}\to 0} \frac{Y_5}{2Y_1 + Y_4} = \frac{-4g^2 A}{4g^2(A+2R_{AB}) + AR_{AB}(A+R_{AB})}. \quad \text{(A6)}$$

[1] Y. Mu and C. M. Savage, Phys. Rev. A **46**, 5944 (1992).
[2] C. Ginzel, H.-J. Briegel, U. Martini, B.-G. Englert, and A. Schenzle, Phys. Rev. A **48**, 732 (1993).
[3] M. Löffler, G. M. Meyer, and H. Walther, Phys. Rev. A **55**, 3923 (1997).
[4] T. Pellizzari and H. Ritsch, J. Mod. Opt. **41**, 609 (1994).
[5] H.-J. Briegel and B.-G. Englert, Phys. Rev. A **47**, 3311 (1993).
[6] H.-J. Briegel, G. M. Meyer, and B.-G. Englert, Phys. Rev. A **53**, 1143 (1996); Europhys. Lett. **33**, 515 (1996).
[7] G. M. Meyer, H.-J. Briegel, and H. Walther, Europhys. Lett. **37**, 317 (1997).
[8] G. M. Meyer, doctoral thesis, University of Munich, 1996 (also as MPQ-Report 221).
[9] G. M. Meyer, M. Löffler, and H. Walther, Phys. Rev. A **56**, R1099 (1997).
[10] P. Horak and K. M. Gheri, Phys. Rev. A **53**, R1970 (1996); K. M. Gheri, P. Horak, and H. Ritsch, J. Mod. Opt. **44**, 605 (1997).
[11] G. M. Meyer and G. Yeoman, Phys. Rev. Lett. **79**, 2650 (1997).
[12] G. Yeoman and G. M. Meyer, Europhys. Lett. **42**, 155 (1998).
[13] H. Steudel and T. Richter, Ann. Phys. (Leipzig) **35**, 122 (1978).
[14] B. R. Mollow, Phys. Rev. **188**, 1969 (1969).
[15] U. Eichmann, J. C. Bergquist, J. J. Bollinger, J. M. Gilligan, W. M. Itano, D. J. Wineland, and M. G. Raizen, Phys. Rev. Lett. **70**, 2359 (1993).
[16] P. Kochan, H. J. Carmichael, P. R. Morrow, and M. G. Raizen, Phys. Rev. Lett. **75**, 45 (1995).
[17] T. Wong, S. M. Tan, M. J. Collett, and D. F. Walls, Phys. Rev. A **55**, 1288 (1997).
[18] H. J. Carmichael and D. F. Walls, J. Phys. B **9**, L43 (1976); H. J. Kimble, M. Dagenais, and L. Mandel, Phys. Rev. Lett. **39**, 691 (1997).
[19] R. G. DeVoe and R. G. Brewer, Phys. Rev. Lett. **76**, 2049 (1996).
[20] J. I. Cirac and P. Zoller, Phys. Rev. Lett. **74**, 4091 (1997).
[21] S. F. Huelga, C. Macchiavello, T. Pellizzari, A. K. Ekert, M. B. Plenio, and I. J. Cirac, Phys. Rev. Lett. **79**, 3865 (1997).
[22] M. O. Scully and K. Drühl, Phys. Rev. A **25**, 2208 (1982).